RESEARCH ARTICLE

WILEY   *Journal of* Cellular Biochemistry

Near-infrared fluorescence-labeled anti-PD-L1-mAb for tumor imaging in human colorectal cancer xenografted mice

Mingyu Zhang[1] | **Huijie Jiang[1]** | **Rongjun Zhang[2]** | **Hao Jiang[1]** | **Hailong Xu[1]** | **Wenbin Pan[1]** | **Xiaolin Gao[3]** | **Zhongqi Sun[1]**

[1]Department of Radiology, The Second Affiliated Hospital of Harbin Medical University, Harbin, China

[2]Jiangsu Institute of Nuclear Medicine, Wuxi, China

[3]Department of Radiology, China-Japan Union Hospital, Jilin University, Changchun, China

Correspondence
Huijie Jiang, Department of Radiology, The Second Affiliated Hospital of Harbin Medical University, No. 246, Xuefu Road, Nangang, Harbin, 150001 Heilongjiang, China.
Email: zmyjhj@163.com
Rongjun Zhang, Jiangsu Institute of Nuclear Medicine, No. 20, Qianrong Road, Wuxi 214063, China.
Email: zhangrongjun@jsinm.org

Abstract

The expression of programmed death ligand-1 (PD-L1) in tumor has been used as a biomarker to predict the anti-PD-L1 immunotherapy response. To develop a noninvasive imaging technique to monitor the dynamic changes in PD-L1 expression in colorectal cancer (CRC), we labeled an anti-PD-L1 monoclonal antibody with near-infrared (NIR) dye and tested the ability of the NIR-PD-L1-mAb probe to monitor the PD-L1 expression in CRC-xenografted mice by performing optical imaging. Consistent with the expression levels of PD-L1 protein in three CRC cell lines in vitro by flow cytometry and Western blot analyses, our in vivo imaging showed the highest fluorescence signal of the xenografted tumors in mice bearing SW620 CRC cells, followed by tumors derived from SW480 and HCT8 cell lines. We detected the highest fluorescent intensity of the tumor at 120 hours after injection of NIR-PD-L1-mAb. The highest fluorescence intensity was seen in the tumor, followed by the spleen and the liver in SW620 xenografted mice. In SW480 and HCT8 xenografted mice, however, the highest fluorescent signals were detected in the spleen, followed by the liver and the tumor. Our findings indicate that SW620 cells express a higher level of PD-L1, and the NIR-PD-L1-mAb binding to PD-L1 on the surface of CRC cells was specific. The technique was safe and could provide valuable information on PD-L1 expression of the tumor for development of a therapeutic strategy of personized targeted immunotherapies as well as treatment response of patients with CRC.

KEYWORDS
colorectal cancer, immunotherapy, noninvasive imaging, optical imaging, programmed death ligand-1/programmed death ligand-1 checkpoint

1 | INTRODUCTION

The T cells are activated by dual signals from specific T cell receptor binding to major histocompatibility complex molecules and from an interaction of the receptors or ligands expressed on the membrane of T cells with the costimulating molecules expressed on the surface of antigen presenting cells (APCs).[1,2] In normal physiological condition, activated

T cells recognize the malignant cells and initiate an antitumor immune response. However, under some circumstances, malignant tumor cells bearing genetic variants express elevated levels of inhibitory receptors and related ligands that suppress T cell activation, resulting in T cell tolerance to tumors and allowing the tumor cells escape immune recognition and avoid immune response.[3-5]

Programmed cell death ligand-1 (PD-L1, B7-H1, or CD274) predominantly expressed on the surface of tumor cells and APCs plays an important role in the inhibition of T cell-mediated immune response.[6] Constitutively overexpressed PD-L1 in several cancers including melanoma, renal cell carcinoma, lung, breast, ovarian, and colorectal cancers (CRC) binds to programmed cell death receptor (PD-1), leading to deactivation of PD-1 expressing T lymphocytes and immune suppression, which is associated with poor prognosis and treatment response.[7] Anti-PD-1/anti-PD-L1 antibodies can prevent the recognition of an important immune checkpoint pathway between PD-1 and PD-L1. Clinical studies have demonstrated anticancer activity of these antibodies in multiple tumor types including advanced melanoma, non–small-cell lung carcinoma, renal cell carcinoma, head and neck cancers, bladder cancer, breast cancer, and Hodgkin's lymphoma.[6,8-10] Therefore, the changes in PD-L1 expression level can be used to monitor the response of anti-PD-1 or anti-PD-L1 immunotherapies. However, more than half of patients with cancer do not respond to checkpoint blockade therapies because of low levels of PD-L1 or PD-1 expression in cancer cells.[11] Furthermore, PD-L1 expression is a dynamic process that can cause a different efficacy and response of anti-PD-1/PD-L1 target therapy among different tumor types and individuals.[12] Thus, there is a pressing clinical demand to accurately determine the expression levels of PD-L1 in vivo and predict which patients are more likely to benefit from immunotherapy.

CRC is one of the most common cancers worldwide, accounting for 10% of all malignancies.[13] It has been reported that upregulation of PD-L1 expression is associated with poor patient's outcomes, and as such positive PD-L1 expression has been considered as an independent predictor for colorectal carcinoma prognosis.[14] While ^{18}F-fluorodeoxygucose positron emission tomography/computer tomography (PET/CT) is routinely used in patients with cancer for staging and disease monitoring, little has been done on the assessment of PD-L1 expression in CRC tumor in vivo. Although immunohistochemistry (IHC) of tumor section could be used to determine the PD-L1 expression, the approach needs an invasive procedure for the biopsy from the patient with the assistance of an endoscope, and may give a false negative-diagnosis because of limitations of IHC-based assessment by core needle biopsy.[6] There were multiple prior attempts to characterize the levels of cell surface PD-L1 in various tumor models.[15] Unfortunately, most of those were unsuccessful because of low and variable levels of PD-L1 expression. Our objective of this study was to develop a noninvasive imaging technique to monitor the dynamic changes in PD-L1 expression in CRC tumor. We labeled an anti-PD-L1 monoclonal antibody with near-infrared (NIR) dye and tested that specificity of the NIR-PD-L1-mAb probe to track PD-L1 expression of CRC cells in vivo by performing optical imaging. Our results demonstrate that noninvasive imaging of monitoring PD-L1 expression in human CRC-xenografted mice is reliable, and the technique could provide valuable information on PD-L1 expression of the tumor for development of therapeutic strategy of personalized immunotherapies as well as treatment response of patients with CRC.

2 | MATERIALS AND METHODS

2.1 | Antibodies and cell lines

Anti-PD-L1 antibody against the extracellular domain of human PD-L1 was purchased from Abcam (EPR19759; Abcam, Cambridge, UK). Anti-GAPDH antibody and peroxidase-conjugated secondary antibody were the products of ZhongShan Golden Bridge Biotech Co (Beijing, China). The human CRC cell lines SW620, SW480, and HCT8 were purchased from the Type Culture Collection of the Chinese Academy of Sciences (Shanghai, China).

2.2 | Animal models

Female BALA/C nude mice (6-8–week old) were purchased from the Animal Laboratory of Cavens Corporate of Changzhou (Changzhou, China). Mice were housed at the animal facility of Jiangsu Institute of Nuclear Medicine under standard approved sterile laboratory conditions. Mice were subcutaneously inoculated in the back with 5.0×10^6 SW620, SW480, and HCT8 cells in 150 μL of phosphate buffered saline (PBS), respectively. When the tumor implants reached 1 cm in diameter (approximately 4 weeks after implantation), the tumor-bearing mice were subjected to in vivo optical tumor imaging and ex vivo biodistribution studies. All procedures were performed with the approval of the Institutional Animal Care and Use Committees of Jiangsu Institute of Nuclear Medicine.

2.3 | Synthesis of NIR-PD-L1-mAb antibody conjugates

Anti-PD-L1-mAb was conjugated with Licor800 dye, by using the IRDye 800CW Protein Labeling Kit from LI-COR, according to the manufacturer's instructions (LI-COR

Biosciences, Lincoln, NE). Briefly, the commercial antibody was first cleaned up with a 3 kDa cutoff Amicon Ultra centrifugal filter (Millipore Corp, Billerica, MA) and washed with the labeling buffer of boric acid solution (pH 8.6) five times. The labeling mixture containing 9 μL of IRDye 800CW NHS Ester in dimethyl sulfoxide, 100 μL of anti-PD-L1-mAb in boric acid solution (pH 8.6) were incubated at 25°C for 2 hours in the dark, followed by desalting with a PD-10 column (Amersham Biosciences, Piscataway, NJ). A Nanodrop 2000 UV-vis spectrophotometer was used to determine the molar extinction coefficient of unlabeled antibody at 280 nm ($\varepsilon_{\mathrm{Protein}}$) and the absorbance of the NIR-PD-L1-mAb at 280 (A_{280}) and 780 nm (A_{780}). The final protein concentration of NIR-PD-L1-mAb and the number of dye molecules per protein molecule (dye/protein ratio) were calculated as the following formula respectively.

$$\text{Protein Conc.(mg/mL)} = \frac{A_{280} - (0.03 \times A_{780})}{\varepsilon_{\mathrm{Protein}}}$$
$$\times MW_{\mathrm{Protein}} \times \text{Dilution Factor,}$$

$$D/P = \left[\frac{A_{780}}{\varepsilon_{\mathrm{Dye}}}\right] \div \left[\frac{A_{280} - (0.03 \times A_{780})}{\varepsilon_{\mathrm{Protein}}}\right].$$

2.4 | Cell culture

The human CRC cell lines SW620, SW480, and HCT8 were maintained in RPMI-1640 supplemented with 10% fetal bovine serum (FBS; Hyclone, Logan, Utah) and 1% penicillin-streptomycin in a humidified atmosphere of 5% CO_2 at 37°C.

2.5 | Flow cytometry

Briefly, cells (1×10^6) were fixed with prechilled 70% alcohol at 4°C for 1 hour, followed by washing with PBS containing 2 mM EDTA and 0.5% FBS. The cells were blocked with goat serum at room temperature for 1 hour and then incubated with anti-human PD-L1 antibody (ab205921; Abcam) or control IgG (ab17273; Abcam) at 1:100 dilution at 4°C overnight. The cells were washed, incubated with Alexa Fluor 488 conjugated anti-rabbit IgG second antibody (ab150077; Abcam) at 1:2000 dilution at room temperature for 2 hours, and analyzed using a FACSCalibur flow cytometer (Becton Dickinson, Franklin, NJ).

2.6 | Western blot analyses

Tumor cells were lysed in RIPA buffer at 4°C for 30 minutes. Aliquots of total cellular proteins (30 μg) were resolved in SDS-PAGE and transferred to polyvinylidene fluoride membranes (Millipore Corp). The membrane was blocked with 5% fat-free milk for 4 hours, and subsequently incubated with primary anti-PD-L1 at 1:100 (ab205921; Abcam) dilution or anti-GAPDH at 1:5000 (ZhongShan Golden Bridge Biotech Co, China) overnight at 4°C, followed by additional incubation with horseradish peroxidase (HRP)-conjugated secondary antibody (ZhongShan Golden Bridge Biotech Co, China) at 1:5000 dilution at room temperature for 1 hour. The specific protein was detected in the presence of HRP substrate luminol reagents by a Bio-Rad ChemiDoc XRS+ imaging system (Bio-Rad, Hercules, CA). Specific protein was quantified by normalizing GAPDH protein using ImageJ software (Java 1.6.0_20, National Institutes of Health).

2.7 | In vivo optical tumor imaging and biodistribution studies

Mice bearing SW620, SW480, or HCT8 tumor were intravenously injected with 200 μL of NIR-PD-L1-mAb (approximately 9.5 μg of protein) under anesthetized with 2% isoflurane gas, and the right lateral position images were acquired with the Pearl Impulse Imager in white light and 800 nm channels (Software v2.0; LI-COR Biosciences) at 24, 48, 72, and 120 hours after injection. Equal-sized regions of interest (ROIs) were drawn on tumors and a nontumor background region. The mean fluorescence intensity value of each tumor was normalized to the background signal, and the ratio of fluorescence intensity of the tumor to background was used for statistical analysis. For biodistribution studies, based on the best time of in vivo imaging, mice were euthanized 5 days after intravenous injection with 200 μL of NIR-PD-L1-mAb. Tumors and selected tissues were harvested and weighed. The mean fluorescence intensity of each organ was measured as described above.

2.8 | Statistical analysis

All data were expressed as the mean ± standard deviation. Statistical analysis was performed using SPSS software version 19 (SPSS, Chicago, IL). The difference between the three groups was assessed using one-way analysis of variance with least-significant difference-test. $P < 0.05$ is considered statistically significant.

3 | RESULTS

3.1 | PD-L1 is expressed at a higher level in SW620 cells than SW480 and HCT8 cell lines

The antibody was labeled with IRDye 800CW NHS Ester by acylating the primary amines of the antibody. The final

protein concentration of NIR-PD-L1-mAb after purification was 47.9 μg/mL, and the dye/protein ratio was 1.954. To determine the binding ability of PD-L1-mAb to PD-L1 expressed on the membrane of colorectal cancer cells in vitro, we examined three cell lines of SW620, SW480, and HCT8 that are known to express various levels of endogenous PD-L1 protein. As shown in Figure 1A and 1B, a higher level of PD-L1 protein expression was detected in SW620 cells than SW480 and HCT8 cells. The average of fluorescence intensity measured by flow cytometry were 18.8 arbitrary units (AU) in SW620 cells, 11.13 AU in SW480 cells, and 7.6 AU in HCT8 cells (Figure 1B). There were significant differences in PD-L1 expression among the three cell lines ($P < 0.001$). To investigate the PD-L1 protein expression in SW620, SW480, and HCT8 cells, we performed Western blot analyses with a specific antibody to human PD-L1. As shown in Figure 2A and 2B, the expression level of PD-L1 in SW620 cells was significantly higher as compared with SW480 or HCT8 cell cells (0.72 ± 0.02 vs 0.52 ± 0.02, and 0.72 ± 0.02 vs 0.45 ± 0.16, respectively; $P < 0.001$). The expression level of PD-L1 protein in SW480 cells was also significantly higher than HCT8 cell line (0.52 ± 0.02 vs 0.45 ± 0.16; $P < 0.01$). This result confirms the diversity of PD-L1 protein expression in three types of CRC cells in vitro, the graded expression was: SW620 > SW480 > HCT8.

3.2 | NIR-PD-L1-mAb specifically accumulates in PD-L1 expressing tumors

To determine whether NIR-PD-L1-mAb could detect the PD-L1 expression in human colorectal cancer cells in vivo, we injected 200 μl of NIR-PD-L1-mAb (approximately 9.5 μg of

protein) into mice bearing SW620, SW480, and HCT8 tumor, respectively, and recorded the tumor imaging profiles at different time-points. We found that the fluorescence could be detected from 24 to 120 hours after injection, and the fluorescent signal became more and more intensive with the time lapse, and grafted tumors could be well displayed at 120 hours (Figure 3). The fluorescence intensity at 120 hours after injection of NIR-PD-L1-mAb was highest in the mice bearing SW620 tumor (9.04 ± 0.28), followed by in mice with SW480 tumor (6.45 ± 0.21), and mice with HCT8 tumor (3.88 ± 0.06).

3.3 | Biodistribution of NIR-PD-L1-mAb in mice bearing SW620 tumor is different from mice with SW480 OR HCT8 xenograft

Fluorescent signals from different freshly dissected tissues were quantified by optical imaging. Figure 4 shows the images of dissected tissues of mice bearing human colorectal cancers that were euthanized 120 hours after injection of NIR-PD-L1-mAb. We noted that fluorescent signals in mice with SW620 tumor at 120 hours was more intensive as compared with the mice with either SW480 or HCT8 xenograft (Figure 4). Consistent with protein expression levels examined by the Western blot in vitro, the highest fluorescence intensity was seen in tumor tissue in SW620 xenograft mouse model (5.05 ± 0.36), followed by the spleen (4.17 ± 0.18), and the liver (3.93 ± 0.13). In SW480 and HCT8 xenograft mice, however, the organs with highest fluorescent signals were detected in the spleen (3.96 ± 0.12 and 4.01 ± 0.07, respectively), followed by the liver (3.81 ± 0.05 and 3.89 ± 0.13, respectively), and
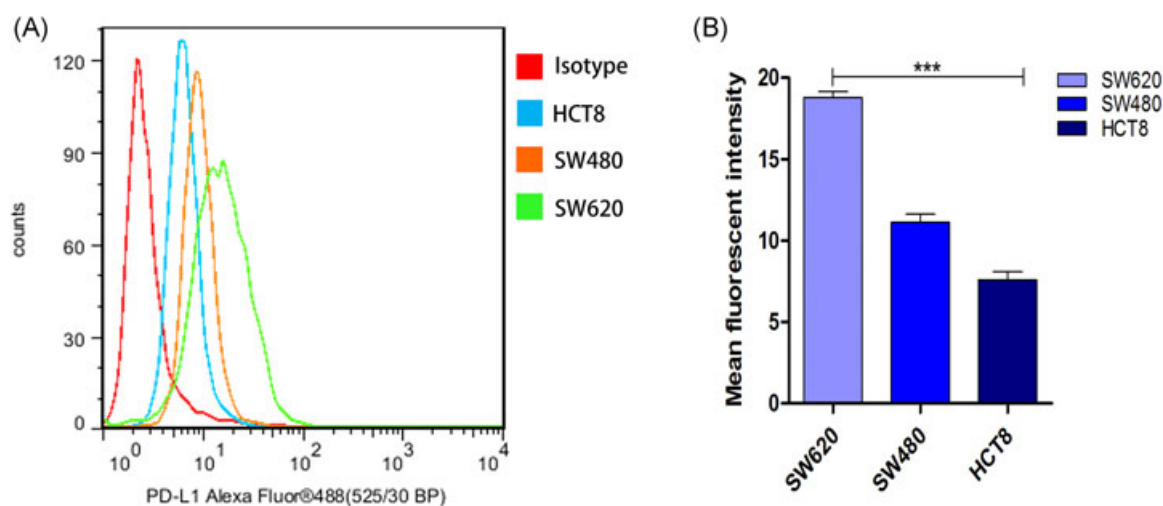
FIGURE 1 NIR-PD-L1-mAb has higher affinity binding to PD-L1 in SW620 cells than SW480 and HCT8 cell lines. Binding affinity of anti-PD-L1 monoclonal antibody to the surface PD-L1 was analyzed by FACS. A, Colorized histograms represent anti-human PD-L1 antibody binding to SW620, SW480 and HCT8 cell lines as indicated. B, Quantification of fluorescent intensity of SW620, SW480, and HCT8 cell lines detected by FACS. Data are expressed as the mean ± standard deviation and the significance of the value is indicated by asterisk, ***$P < 0.001$ ($n = 3$). NIR, near-infrared; PD-L1, programmed death ligand-1

(A)

SW620   SW480   HCT8

PD-L1

GAPDH

(B)

SW620
SW480
HCT8

PD-L1/GAPDH

0.8
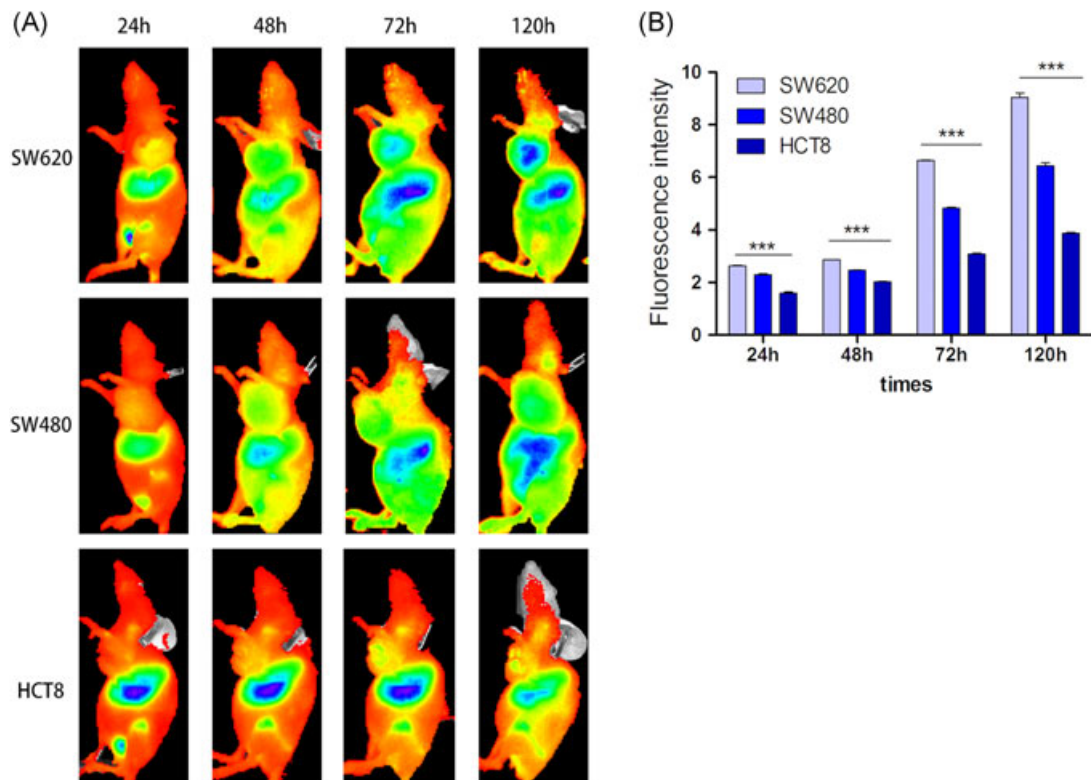0.6
0.4
0.2
0.0

***
**
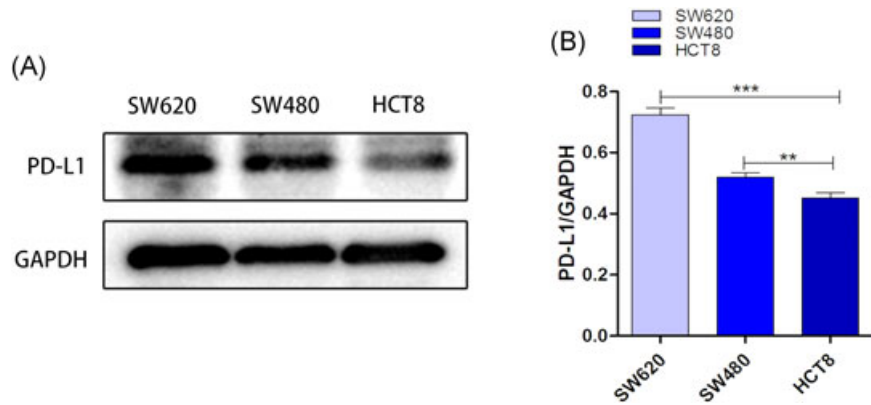
SW620   SW480   HCT8

FIGURE 2 Comparison of PD-L1 protein expression levels between SW620, SW480, and HCT8 cells in vitro. A, PD-L1 expression in SW620, SW480, and HCT8 cells measured by the Western blot. B, Quantification of Western blot analyses. Data are expressed as the mean $\pm$ standard deviation and the significance of the value is indicated by an asterisk, ***$P < 0.001$, **$P < 0.01$ ($n = 3$). PD-L1, programmed death ligand-1

tumor tissues (3.70 ± 0.10 and 2.99 ± 0.05, respectively). The relative fluorescence intensity (T/B) in the three xenograft models of SW620, SW480, and HCT8 were 5.05 ± 0.36, 3.70 ± 0.10, and 2.99 ± 0.05, respectively. The retention of NIR-PD-L1-mAb in the kidneys in mice with SW620 tumor seemed higher as compared with the other two grafted mice.

4 | DISCUSSION

With the development of personalized therapy, more and more people gain survival benefit from PD-1/PD-L1-targeted immunotherapies. Recent studies demonstrated that tumors expressing high levels of PD-L1 in infiltrating immune cells had a better response to immunotherapies

(A)   24h   48h   72h   120h

SW620

SW480

HCT8

(B)

Fluorescence intensity

10
8
6
4
2
0

SW620
SW480
HCT8

***   ***   ***   ***

24h   48h   72h   120h
times

FIGURE 3 NIR-PD-L1-mAb specifically binds to PD-L1 in human colorectal cancer xenografted mice. A, Optical images in SW620, SW480, and HCT8 grafted mice at different time-points. B, Quantitative fluorescent intensity of optical imaging regions of interest (ROIs) of tumor to background at 24, 48, 72, and 120 hours, respectively after injection of NIR-PD-L1-mAb ($n = 3$). Data are expressed as the mean $\pm$ standard deviation of the fluorescence intensity ratio of tumor to background. The significance of the value is indicated by an asterisk, ***$P < 0.001$. NIR, near-infrared; PD-L1, programmed death ligand-1
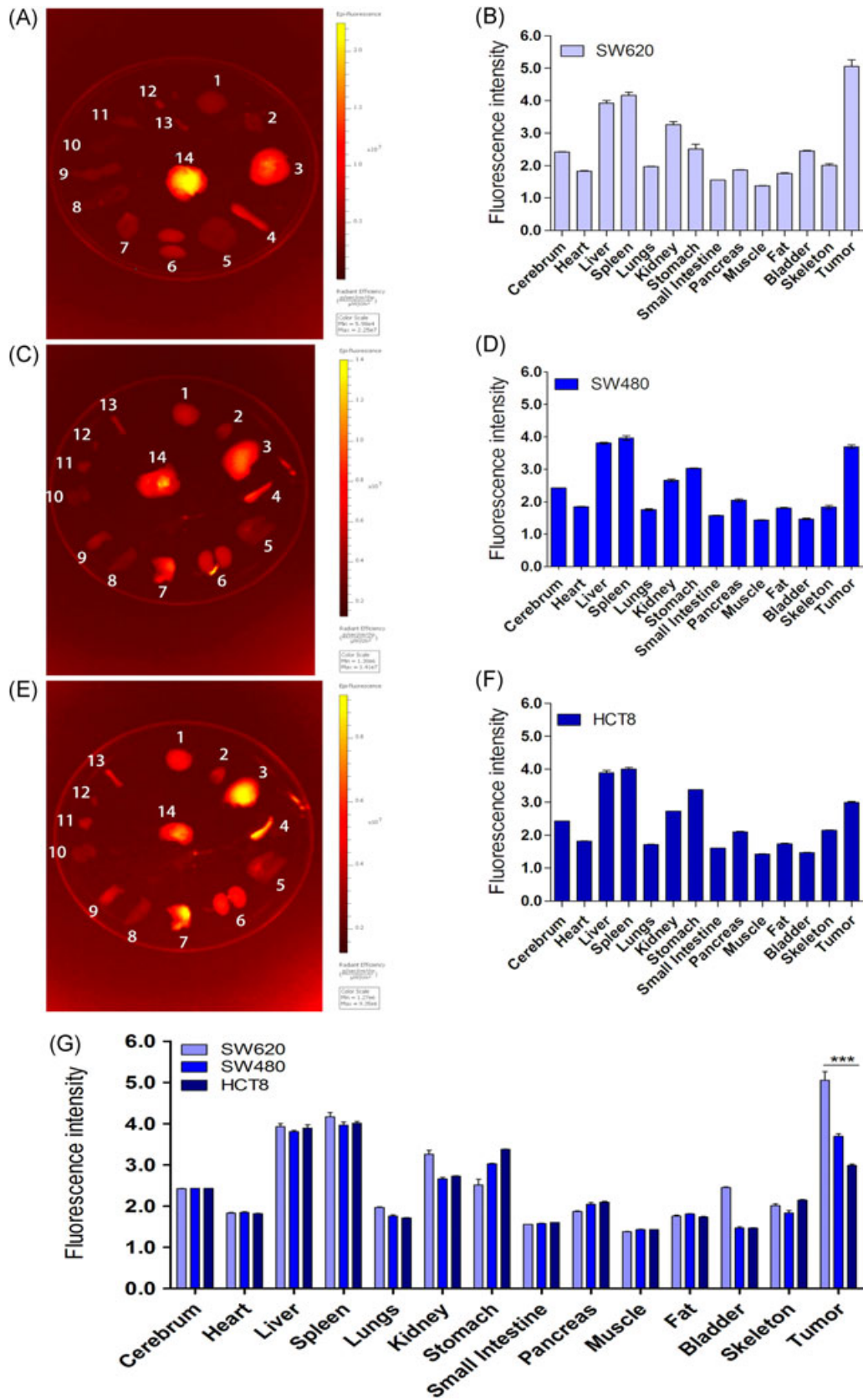
FIGURE 4 Continued.

in some patients.[16,17] For example, Topalian et al[18] reported that nine of 25 patients with PD-L1-expressing tumors responded to PD-1/PD-L1 blockage while none of 17 patients with PD-L1 nonexpressing tumors responded. Further study showed that the responses were also observed in PD-L1 negative cancers although to a much lesser extent because of the effect of PD-1/PD-L1 blockade on the heterogeneity of PD-L1 expression in cancer lesions.[18] A study by Wang et al[19] indicated that PD-L1-positive expression in tumor cells was associated with worse clinical outcome for patients with CRC. Further research revealed that a small subgroup of metastatic CRC patients with deficiency in mismatch repair do respond to atezolizumab (a PD-L1-targeted mAb approved by FDA) immunotherapies.[20] These studies raise an important question as to how PD-L1 expression is correctly assessed since IHC-based assay by core needle biopsy may not truly reflect the PD-L1 expression status because of IHC limitations under some circumstances such as heterogeneous PD-L1 expression in the tumor, PD-L1 expression outside of the tumor and its dynamic changes in PD-L1 expression over the tumor progression, and different thresholds for positivity applied in different laboratories.[6] Thus it is in great demand to develop a molecular imaging that can noninvasively monitor the dynamic expressions of PD-L1 in vivo to overcome the spatial, temporal and heterogeneity errors caused by IHC on single or repeated biopsies.[21]

Over the past several years, NIR fluorescence intraoperative imaging has been used to guide surgery to assess the adequate resection margins for narrowing the gap between preoperative imaging and intraoperative reality.[22] This novel technique has been increasingly used in the resecting variety of cancers, including colorectal cancer and colorectal liver metastases.[23,24] Recently, NIR-conjugated antibodies have been widely used to monitor the expression levels of tumor-specific antigens.[25] PET imaging is also considered to be a promising technology for noninvasive imaging. However, radiolabeled anti-PD-L1 antibodies depend on the long half-life of radionuclide and labeling procedure is more complex. Compared with radiolabeled antibody-based PET imaging, NIR-based optical imaging can satisfy longer clearance times and

the labeling procedure is easier. In the present study, we synthesized and applied a NIR-labeled human monoclonal antibody specific to PD-L1 to measure PD-L1 expressions of human CRC in subcutaneous xenografted mice via optical imaging. We also optimized the timepoint for NIR-PD-L1-mAb imaging in tumor grafted mice. Our studies demonstrated that the NIR-PD-L1-mAb binding to PD-L1 on the surface of CRC cells was specific as evidenced by its ability to detect various levels of PD-L1 expression in CRC-xenografted models. Consistent with the expression levels of PD-L1 protein in three CRC cell lines in vitro, our in vivo imaging approach detected the highest fluorescence signal of the xenografted tumors in mice bearing SW620 CRC cells, followed by tumors derived from SW480 and HCT8 cell lines. The SW620 cells appear more aggressive and express a much higher level of PD-L1 protein than other two cell lines since they were derived from the metastatic lymph nodes of colorectal adenocarcinoma while the SW480 and HCT8 cell lines were derived from colorectal carcinoma in situ.[14]

In agreement with other investigators, we detected the highest fluorescent intensity in the grafted tumor at 120 hours after injection of NIR-PD-L1-mAb.[26] In contrast to our observation, however, Truillet et al[27] found the best time for detection of PD-L1 expression in vivo at 48 hours after injection of ^{89}Zr-C4. The possible explanation of the difference in optimal time of PD-L1 detection between Tuillet's observation and ours was because of the advantage of small molecular weight of C4. The C4 molecule is an engineered single-stranded monoclonal antibody that contains fused variable Fabs fragments specific to PD-L1 antigen, while NIR-PD-L1-mAb is an intact IgG molecule produced in mouse cells that has a relatively slow circulation clearance as reported in other studies.[15] In addition, our biodistribution analyses showed a significant difference among three types of CRC-xenografted mice at 120 hours after injection of NIR-PD-L1-mAb. The highest fluorescent accumulation was seen in SW620 grafted tumors, which agreed with the higher level of protein expression data from the flow cytometry and Western blot analyses. We also detected high fluorescent accumulation in the spleen in SW620 model, as well as in SW480 and HCT8 models at

FIGURE 4 Ex vivo optical biodistribution at 120 hours after injection of NIR-PD-L1-mAb in SW620, SW480, and HCT8 xenograft models. A, B, Optical biodistribution image and corresponding quantitative data of SW620 grafted mice. C, D, Optical biodistribution image and corresponding quantitative data of SW480 grafted mice. E, F, Optical biodistribution image and corresponding quantitative data of HCT8 grafted mice. G, Histograms of biodistribution fluorescent accumulation in SW620, SW480, and HCT8 grafted mice, respectively. Data are expressed as the mean ± standard deviation of the fluorescent intensity ratio of tumor to background. The significance of the value is indicated by an asterisk, ***$P < 0.001$ ($n = 3$) by one-way ANOVA. ANOVA, analysis of variance; NIR, near-infrared; PD-L1, programmed death ligand-1

120 hours after the probe injection. Our studies together with previous immuno-SPECT/PET studies suggest that the spleen tissue express a higher level of endogenous PD-L1 than grafted SW480 or HCT8 tumors.[28-30] Our findings indicate that NIR-PD-L1-mAb can specifically detect the PD-L1 expression, and possibly the heterogeneity of PD-L1 expression of human CRC tumor cells too, to guide PD-1/PD-L1-targeted immunotherapies. They also support future work on the use of PD-L1-targeted molecular imaging agents combined with other biomarkers to better guide the PD-1/PD-L1-targeted therapeutic strategy of personized targeted immunotherapies and response to anti-PD-L1 treatment in patients with CRC.

In this study, we chose female mice because previous studies have shown that estrogen has protective effects against ischemia/reperfusion injury and protects some organs, as such females can improve the success rate in transplantation experiments. In addition, male rats are more aggressive and often fight each other, which may lead to the injury and compromise the results. However, whether the NIR-PD-L1-mAb also binds to the PD-L1 on the surface of grafted CRC cells with the same affinity and distributes the same way in males as in females needs to be studied in future. We chose the best time-point of NIR-PD-L1-mAb imaging on the 5th day (eg 120 hours) after a single injection because we found that the fluorescence intensity began to decrease dramatically after the 6th day. Our future work will monitor changes in PD-L1 protein expression of anticancer drug-treated tumors in the xenografted animal models over extended periods of multiple time-points after multiple injections by using NIR-PD-L1 optical imaging.

In conclusion, we developed a NIR dye-labeled anti-PD-L1 monoclonal antibody that is feasible to noninvasively monitor PD-L1 expression in vivo with optical imaging and demonstrated a noninvasive imaging technique to monitor and assess dynamic PD-L1 expression in human CRC tumor microenvironment. Our findings provided valuable diagnostic information for PD-1/PD-L1-targeted immunotherapy selection and treatment response assessment in patients with CRC in future clinical practice of anti-PD-L1-mAb based imaging.

CONFLICTS OF INTEREST

The authors declare that there are no conflicts of interest.

ORCID

Huijie Jiang https://orcid.org/0000-0003-1927-2674

REFERENCES

1. Le Mercier I, Lines JL, Noelle RJ. Beyond CTLA-4 and PD-1, the generation Z of negative checkpoint regulators. *Front Immunol.* 2015;6:418. https://doi.org/10.3389/fimmu.2015.00418
2. Honda T, Egen JG, Lämmermann T, Kastenmüller W, Torabi-Parizi P, Germain RN. Tuning of antigen sensitivity by T cell receptor-dependent negative feedback controls T cell effector function in inflamed tissues. *Immunity.* 2014;40(2):235-247. https://doi.org/10.1016/j.immuni.2013.11.017
3. Topalian SL, Drake CG, Pardoll DM. Immune checkpoint blockade: a common denominator approach to cancer therapy. *Cancer Cell.* 2015;27(4):450-461. https://doi.org/10.1016/j.ccell.2015.03.001
4. Dunn GP, Bruce AT, Ikeda H, Old LJ, Schreiber RD. Cancer immunoediting: from immuno-surveillance to tumor escape. *Mat Immunol.* 2002;3:991-998.
5. Gubin MM, Zhang X, Schuster H, et al. Checkpoint blockade cancer immunotherapy targets tumour-specific mutant antigens. *Nature.* 2014;515(7528):577-581. https://doi.org/10.1038/nature13988
6. Wang X, Teng F, Kong L, Yu J. PD-L1 expression in human cancers and its association with clinical outcomes. *Onco Targets Ther.* 2016;9:5023-5039. https://doi.org/10.2147/ott.s105862
7. Wu P, Wu D, Li L, Chai Y, Huang J. PD-L1 and survival in solid tumors: a meta-analysis. *PLOS One.* 2015;10(6):e0131403. https://doi.org/10.1371/journal.pone.0131403
8. Li JH, Zhu Y, Yang J, Qin LX. The progress in tumor immune checkpoint-targeted immunotherapy. *Fudan Univ J Med Sci.* 2016;43(1):110-114.
9. Kantoff Philip W, Higano CS, Shore ND. Sipuleucel-T immunotherapy for castration-resistant prostate cancer. *N Engl J Med.* 2010;363(5):411-422.
10. Salama AK, Gangadhar T. Clinical applications of PD-1-based therapy: a focus on pembrolizumab (MK-3475) in the management of melanoma and other tumor types. *Onco Targets Ther.* 2015;8:929-937. https://doi.org/10.2147/ott.s53164
11. Schumacher TN, Kesmir C, Van buuren MM. Biomarkers in cancer immunotherapy. *Cancer Cell.* 2015;27(1):12-14. https://doi.org/10.1016/j.ccell.2014.12.004
12. Teng F, Meng X, Kong L, Yu J. Progress and challenges of predictive biomarkers of anti PD-1/PD-L1 immunotherapy: a systematic review. *Cancer Lett.* 2018;414:166-173. https://doi.org/10.1016/j.canlet.2017.11.014
13. Torre LA, Bray F, Siegel RL, Ferlay J, Lortet-Tieulent J, Jemal A. Global cancer statistics, 2012. *CA Cancer J Clin.* 2015;65(2):87-108. https://doi.org/10.3322/caac.21262
14. Shi SJ, Wang LJ, Wang GD, et al. B7-H1 expression is associated with poor prognosis in colorectal carcinoma and regulates the proliferation and invasion of HCT116 colorectal

cancer cells. *PLOS One.* 2013;8(10):e76012. https://doi.org/10.1371/journal.pone.0076012

15. Heskamp S, Hobo W, Molkenboer-Kuenen JDM, et al. Non-invasive imaging of tumor PD-L1 expression using radiolabeled anti-PD-L1 antibodies. *Cancer Res.* 2015;75(14):2928-2936. https://doi.org/10.1158/0008-5472.can-14-3477

16. Yang J, Riella LV, Chock S, et al. The novel costimulatory programmed death ligand 1/B7.1 pathway is functional in inhibiting alloimmune responses in vivo. *J Immunol.* 2011;187(3):1113-1119. https://doi.org/10.4049/jimmunol.1100056

17. Herbst RS, Soria JC, Kowanetz M, et al. Predictive correlates of response to the anti-PD-L1 antibody MPDL3280A in cancer patients. *Nature.* 2014;515(7528):563-567. https://doi.org/10.1038/nature14011

18. Topalian SL, Hodi FS, Brahmer JR, et al. Safety, activity, and immune correlates of anti-PD-1 antibody in cancer. *N Engl J Med.* 2012;366(26):2443-2454. https://doi.org/10.1056/NEJMoa1200690

19. Wang L, Ren F, Wang Q, et al. Significance of programmed death ligand 1 (PD-L1) immunohistochemical expression in colorectal cancer. *Mol Diagn Ther.* 2016;20(2):175-181. https://doi.org/10.1007/s40291-016-0188-1

20. Tapia Rico G, Price TJ. Atezolizumab for the treatment of colorectal cancer: the latest evidence and clinical potential. *Expert Opin Biol Ther.* 2018;18(4):449-457. https://doi.org/10.1080/14712598.2018.1444024

21. Ehlerding EB, England CG, McNeel DG, Cai W. Molecular imaging of immunotherapy targets in cancer. *J Nucl Med.* 2016;57(10):1487-1492. https://doi.org/10.2967/jnumed.116.177493

22. Vahrmeijer AL, Hutteman M, van der Vorst JR, van de Velde CJH, Frangioni JV. Image-guided cancer surgery using near-infrared fluorescence. *Nat Rev Clin Oncol.* 2013;10(9):507-518. https://doi.org/10.1038/nrclinonc.2013.123

23. van der Vorst JR, Schaafsma BE, Hutteman M, et al. Near-infrared fluorescence-guided resection of colorectal liver metastases. *Cancer.* 2013;119(18):3411-3418. https://doi.org/10.1002/cncr.28203

24. Verbeek FPR, van der Vorst JR, Tummers QRJG, et al. Near-infrared fluorescence imaging of both colorectal cancer and ureters using a low-dose integrin targeted probe. *Ann Surg Oncol.* 2014;21(suppl 4):S528-S537. https://doi.org/10.1245/s10434-014-3524-x

25. Oliveira S, van Dongen GAMS, Walsum MS, et al. Rapid visualization of human tumor xenografts through optical imaging with a near-infrared fluorescent anti-epidermal growth factor receptor nanobody. *Mol Imaging.* 2012;11(1):7290.2011.00025. 7290.2011.00025. https://doi.org/10.2310/7290.2011.00025

26. Chatterjee S, Lesniak WG, Gabrielson M, et al. A humanized antibody for imaging immune checkpoint ligand PD-L1 expression in tumors. *Oncotarget.* 2016;7(9):10215-10227.

27. Truillet C, Oh HLJ, Yeo SP, et al. Imaging PD-L1 expression with immunoPET. *Bioconjug Chem.* 2018;29(1):96-103. https://doi.org/10.1021/acs.bioconjchem.7b00631

28. Josefsson A, Nedrow JR, Park S, et al. Imaging, biodistribution, and dosimetry of radionuclide-labeled PD-L1 antibody in an immunocompetent mouse model of breast cancer. *Cancer Res.* 2016;76(2):472-479. https://doi.org/10.1158/0008-5472.can-15-2141

29. Natarajan A, Mayer AT, Xu L, Reeves RE, Gano J, Gambhir SS. Novel radiotracer for immunoPET imaging of PD-1 checkpoint expression on tumor infiltrating lymphocytes. *Bioconjug Chem.* 2015;26(10):2062-2069. https://doi.org/10.1021/acs.bioconjchem.5b00318

30. Hettich M, Braun F, Bartholomä MD, Schirmbeck R, Niedermann G. High-resolution PET imaging with therapeutic antibody-based PD-1/PD-L1 checkpoint tracers. *Theranostics.* 2016;6(10):1629-1640. https://doi.org/10.7150/thno.15253